Diffusive and localization behavior of electromagnetic waves in a two-dimensional random medium

Ken Kang-Hsin Wang* and Zhen Ye†
Wave Phenomena Laboratory and Center of Complex Systems, Department of Physics, National Central University, Chungli, Taiwan 32054, Republic of China
(Received 2 June 2003; published 22 October 2003)

In this paper, we discuss the transport phenomena of electromagnetic waves in a two-dimensional random system which is composed of arrays of electrical dipoles, following the model presented earlier by Erdogan *et al.* [J. Opt. Soc. Am. B **10**, 391 (1993)]. A set of self-consistent equations is presented, accounting for the multiple scattering in the system, and is then solved numerically. A strong localization regime is discovered in the frequency domain. The transport properties within, near the edge of, and nearly outside the localization regime are investigated for different parameters such as filling factor and system size. The results show that within the localization regime, waves are trapped near the transmitting source. Meanwhile, the diffusive waves follow an intuitive but expected picture. That is, they increase with traveling path as more and more random scattering incurs, followed by a saturation, then start to decay exponentially when the travelling path is large enough, signifying the localization effect. For the cases where the frequencies are near the boundary of or outside the localization regime, the results of diffusive waves are compared with the diffusion approximation, showing less encouraging agreement as in other systems [Asatryan *et al.*, Phys. Rev. E **67**, 036605 (2003)].

DOI: 10.1103/PhysRevE.68.046608 PACS number(s): 42.25.Hz, 41.90.+e

I. INTRODUCTION

Waves are a ubiquitous phenomenon that is relevant to our everyday life. Our knowledge about nature is mainly obtained through either acoustic or electromagnetic waves. When waves propagate through a random medium, some peculiar properties emerge and some of them have stood as a long outstanding problem for physicists. The most intriguing and still unsolved puzzle perhaps is the so-called Anderson localization. The concept of Anderson localization was initially proposed nearly half a century ago for the possible phenomenon of disorder-induced metal-insulator transition in electronic systems [1]. To make it simple, Anderson localization refers to situations where electrons, when released in a random medium which could be, for instance, a free space with random potentials, may stay close to the initial place. The envelope of the electronic wave function subsequently is revealed as an exponential decay along any direction from the emitting point [2]; the length measuring the e-fold decay is called the localization length. The mechanism behind this property has been attributed purely to sufficient multiple scattering of electrons by the random potentials, a feature of the wave nature of electrons.

Since its inception, the localization concept has opened a wide door for scientists from various backgrounds, and stimulated a vast body of research. The fact that electronic localization is due to the wave nature of electrons is particularly important, as the concept may also be applied to classical wave systems by analogy [3]. The concept of localization has far reached many fields such as seismology [4], oceanology [5], and random lasers [6], to name just a few. The great efforts have been summarized in a number of reviews (e.g., Refs. [2,7–13]).

Over the past two decades, localization of electromagnetic and acoustic waves has been and continues to be a particularly attracting problem, leading to a great amount of publications (e.g., Refs. [8–10,14–28]). The theory of classical waves has been detailed in the textbook [9]. In spite of the tremendous efforts, however, there are still some open questions for wave localization in two-dimensional (2D) random systems. For example, one of them concerns with the transport behavior of waves within and outside localization regimes. It has been discussed much in the literature that within the localization regime the wave intensity follows a diffusive behavior for transport path smaller than localization length, whereas it follows an exponential decay when the path is greater than the localization length [9,29]. In addition, it has been conjectured that all waves are bound to be localized in 2D for any given amount of disorders or randomness [30], a conclusion significantly influencing nearly all later investigations. If this general hypothesis is true, one would expect that the wave intensity would have to follow the diffusion to localization transition as the transport distance increases although such a transition has not been solidly confirmed yet, to the best of knowledge. Recent studies, however, tend to suggest that this conjecture may not be generally valid [31,32]. On one hand, in Ref. [31] it has been suggested that acoustic waves could not be localized in certain frequency ranges, as would have been expected. On the other hand, the research reported in Ref. [32] reveals different frequency regimes of electromagnetic (EM) wave transport. In certain ranges, the wave transport behavior can be entirely described by the usual Boltzmann-diffusion approximate theory, while in others the behavior does not perform a diffusive feature. The authors called the latter phenomenon anomalous diffusion, and interpreted it as the incipience of Anderson localization. These works seem to uncover that as the frequency varies, there will be a transition between lo-

*Present address: Department of Physics, University of Rochester, Rochester, NY 14627, USA.
†Electronic address: zhen@phy.ncu.edu.tw

calization and nonlocalization in two-dimensional disordered media. Whether these observations also hold in a general perspective, however, remains to be known.

The difficulties in the study of possible nonlocalization or localization of EM waves mainly lie in a number of problems. First, wave localization only appears for strongly scattering media, and such a medium is often hard to find. Second, localization effects are often entangled with other effects such as dissipation, wave deflection, or boundary effects [13], making data interpretation possibly ambiguous. Third, in spite of the fact that many two-dimensional systems are exactly solvable by numerical computation, the simulation is very time consuming and is obviously limited by computing facilities with regard to some unavoidable problems such as finite size. How to find a suitable model that could ease these concerns poses a challenging problem in its own right.

In a recent communication, a simple but seemingly realistic model system has been proposed to study EM localization in 2D random media [33]. This model originated from the previous study of the radiative effects of the electric dipoles embedded in structured cavities [34]. It was shown that EM localization is possible in such a disordered system. When localization occurs, a coherent behavior appears and is revealed as a unique property differentiating localization from either the residual absorption or the attenuation effects.

In the present paper, we wish to explore further the transport properties of the system outlined in Ref. [33]. The advantage of this system not only rests on its simplicity but also on its relatively less time consumption. It has been shown that there is a strong localization region in the system. We will investigate the transport behavior of wave intensity within, near the edge of, and outside the strong localization regime. We study how the transport behavior depends on scatterer's filling parameter, frequency, sample size and so on. When the localization effect is less obvious, we compare the numerically evaluated wave intensity with the result from the diffusion theory.

The paper is structured as follows. The description of the system and the relevant theoretical modeling are presented in the following section, followed by the numerical simulation and detailed discussion of results. A summary concludes the paper in the last section.

II. THE SYSTEM AND THEORETICAL FORMULATION

Here we present the system and the theoretical formulation. Although these have already been presented before [35], for the sake of convenience on the reader's part and easy discussion on our part, we purposely repeat the essence here.

A. The system

Following Erdogan *et al.* [34], we consider 2D dipoles as an ensemble of harmonically bound charge elements. In this way, each 2D dipole is regarded as a single dipole line, characterized by the charge and dipole moment per unit length. Assume that N parallel dipole lines, aligned along the z axis, are embedded in a uniform dielectric medium and *randomly* located at $\vec{r}_i$ $(i=1,2,\ldots,N)$. The averaged distance between dipoles is d. A stimulating dipole line source is located at $\vec{r}_s$, transmitting a continuous wave of angular frequency ω. By the geometrical symmetry of the system, we only need to consider the z component of the electrical waves.

B. The formulation

Although much of the following materials can be referred to in Ref. [33], we repeat the important parts here for the sake of convenience and completeness.

Upon stimulation, each dipole will radiate EM waves. The radiated waves will then repeatedly interact with the dipoles, forming a process of multiple scattering. The equation of motion for the ith dipole is

$$\frac{d^2}{dt^2}p_i+\omega_{0,i}^2 p_i=\frac{q_i^2}{m_i}E_z(\vec{r}_i)-b_{0,i}\frac{d}{dt}p_i \quad \text{for} \quad i=1,2,\ldots,N, \tag{1}$$

where $\omega_{0,i}$ is the resonance (natural) frequency; p_i, q_i, and m_i the dipole moment, charge, and effective mass per unit length of the ith dipole, respectively. $E_z(\vec{r}_i)$ is the total electrical field acting on dipole p_i, which includes the radiated field from other dipoles and also the directly field from the source. The factor $b_{0,i}$ denotes the damping due to energy loss and radiation, and can be determined by energy conservation. Without energy loss (such as heat), $b_{0,i}$ can be determined from the balance between the radiative and vibrational energies, and is given as [34]

$$b_{0,i}=\frac{q_i^2\omega_{0,i}}{4\epsilon m_i c^2}, \tag{2}$$

with ϵ being the permittivity constant and c the speed of light in the medium separately.

Equation (1) is virtually the same as Eq. (1) in Ref. [34]. The only difference is that in Ref. [34], E_z is the reflected field at the dipole due to the presence of reflecting surrounding structures, while in the present case the field is from the stimulating source and the radiation from all other dipoles.

The transmitted electrical field from the continuous line source is determined by the Maxwell equations [34]

$$\left(\nabla^2-\frac{\partial^2}{c^2\partial t^2}\right)G_0(\vec{r}-\vec{r}_s)=-4\mu_0\omega^2 p_0\pi\delta^{(2)}(\vec{r}-\vec{r}_s)e^{-i\omega t}, \tag{3}$$

where ω is the radiation frequency and p_0 is the source strength and is set to be unity. The solution of Eq. (3) is clearly

$$G_0(\vec{r}-\vec{r}_s)=(\mu_0\omega^2 p_0)i\pi H_0^{(1)}(k|\vec{r}-\vec{r}_s|)e^{-i\omega t}, \tag{4}$$

with $k=\omega/c$ and $H_0^{(1)}$ being the zeroth-order Hankel function of the first kind.

Similarly, the radiated field from the ith dipole is given by

$$\left(\nabla^2 - \frac{\partial^2}{c^2 \partial t^2}\right) G_i(\vec{r}-\vec{r}_i) = \mu_0 \frac{d^2}{dt^2} p_i \delta^{(2)}(\vec{r}-\vec{r}_i). \quad (5)$$

The field arriving at the ith dipole is composed of the direct field from the source and the radiation from all other dipoles, and thus is given as

$$E_z(\vec{r}_i) = G_0(\vec{r}_i - \vec{r}_s) + \sum_{j=1, j\neq i}^{N} G_j(\vec{r}_i - \vec{r}_j). \quad (6)$$

Substituting Eqs. (4), (5), and (6) into Eq. (1), and writing $p_i = p_i e^{-i\omega t}$, we arrive at

$$(-\omega^2 + \omega_{0,i}^2 - i\omega b_{0,i}) p_i = \frac{q_i^2}{m_i}\left[G_0(\vec{r}_i - \vec{r}_s) + \sum_{j=1, j\neq i}^{N} \frac{\mu_0 \omega^2}{4} i H_0^{(1)}(k|\vec{r}_i - \vec{r}_j|) p_j \right]. \quad (7)$$

This set of linear equations can be solved numerically for p_i. After p_i are obtained, the total field at any space point can be readily calculated from

$$E_z(\vec{r}) = G_0(\vec{r} - \vec{r}_s) + \sum_{j=1}^{N} G_j(\vec{r} - \vec{r}_j). \quad (8)$$

In the standard approach to wave localization, waves are said to be localized when the square modulus of the field $|E(\vec{r})|^2$, representing the wave energy, is spatially localized after the trivial cylindrically spreading effect is eliminated. Obviously, this is equivalent to, say, that the further away is the dipole from the source, the smaller is its oscillation amplitude, and the decay is expected to follow an exponentially decreasing pattern.

An alternative two-dimensional dipole model was devised previously by other authors [22]. There, the authors derived a set of linear algebraic equations, which is similar in form to the above Eq. (6). However, the fundamental difference between the two models is with respect to the relation between the incident and the scattered waves. In Ref. [22], the interaction between dipoles and the external field is derived by the energy conservation, while in the present case the coupling is determined without ambiguity by the Newton's second law. The former leads to an undetermined phase factor. According to, e.g., Refs. [34,36], the energy conservation can give the radiation factor in Eq. (2).

There are several ways to introduce randomness to Eq. (7). For example, the disorder may be introduced by randomly varying properties of individual dipoles such as the charge, the mass, or the two combined. This is the most common way by which the disorder is introduced into the tight-binding model for electronic waves [37]. In the present study, the disorder is brought in by the random spatial distribution of the dipoles.

For simplicity yet without losing generality, assume that all the dipoles are identical and they are randomly distributed within a certain area. The source is located at the center (set to be the origin) of this area. For convenience, we make Eq. (7) non-dimensional by scaling the frequency by the resonance frequency of a single dipole ω_0. This will lead to two independent nondimensional parameters $b = q^2\mu_0/4m$ and $b_0' = (\omega/\omega_0)(b_0/\omega_0)$. Both parameters may be adjusted in the experiment. For example, the factor b_0 can be modified by coating layered structures around the dipoles [34]. Then Eq. (7) becomes simply

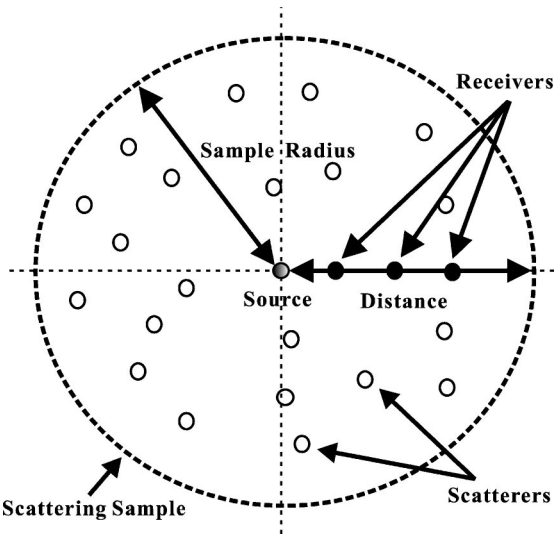

FIG. 1. Conceptual layout of the system and the simulation.

$$(-f^2 + 1 - ib_0')p_i = ibf^2\left[p_0 H_0^{(1)}(k|\vec{r}_i - \vec{r}_s|) + \sum_{j=1, j\neq i}^{N} p_j H_0^{(1)}(k|\vec{r}_i - \vec{r}_j|) \right] \quad (9)$$

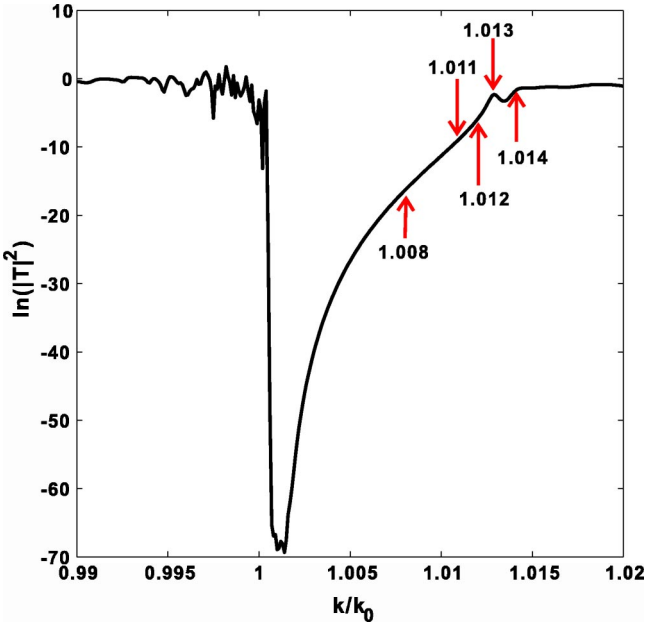

FIG. 2. The transmission vs the reduced frequency. Here the number of dipoles is 1964 and the radius of the sample is 10 unit length; this amounts to a filling of about 6.25.

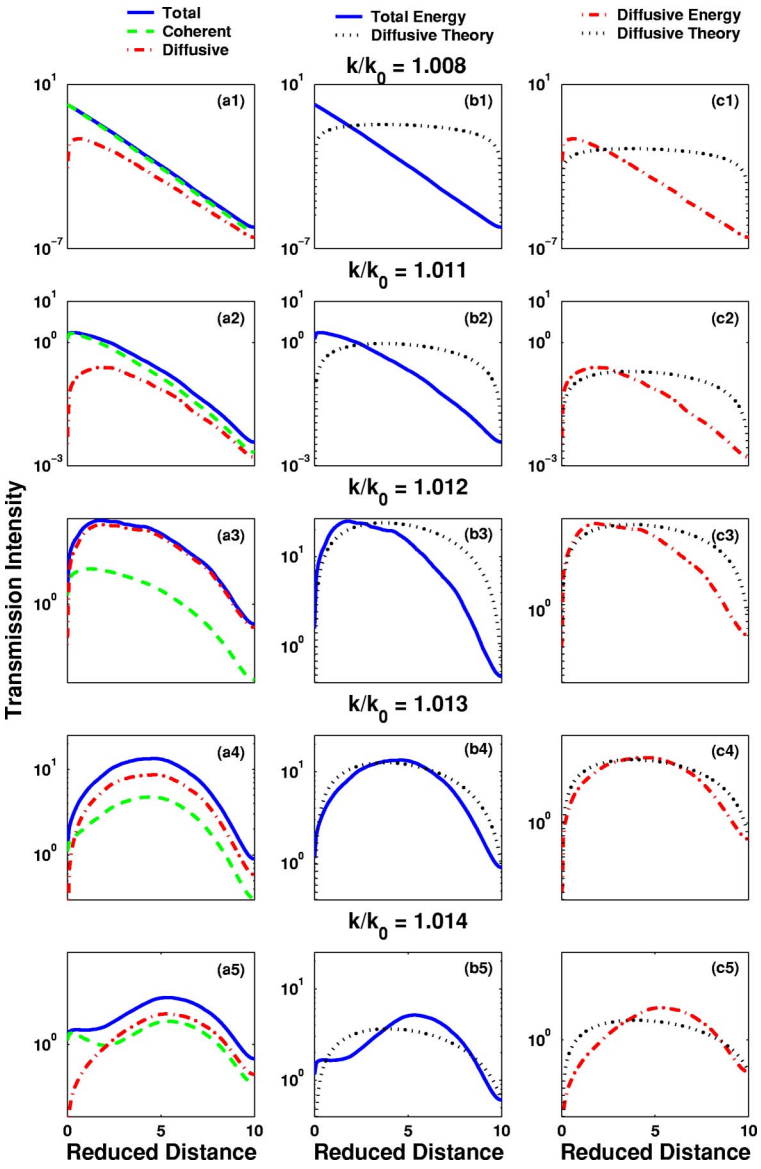

FIG. 3. Transport behavior for a fixed sample size: (a) the total, coherent, and diffusive intensity as a function of the dimensionless traveling distance; (b) the comparison of the numerical results of the total energy with that from the diffusion theory; (c) the comparison of the numerical results of the diffusive energy with that from the diffusion theory. We considered 1964 dipoles to form a sample whose radius is roughly 10. Hereafter, the ''reduced distance'' along the x axis refers to the distance scaled by l, as defined in the text.

with $f=\omega/\omega_0$. Equation (9) is self-consistent and can be solved numerically for p_i and then the total field is obtained through Eqs. (3), (5), and (8).

C. Expected transport behavior

1. In general

Following Ref. [38], a general consideration of the spatial behavior of wave transport is possible. Consider a wave transmitted in a random medium. The transport equation for the total energy intensity I, i.e., $\langle|E|^2\rangle$, may be intuitively written as

$$\frac{dI}{dx}=-\alpha I, \tag{10}$$

where α represents decay along the path traversed. After penetrating into the random medium, the wave will be scattered by random inhomogeneities. As a result, the wave coherence starts to decrease, yielding the way to incoherence. Extinction of the coherent intensity I_C, i.e., $|\langle E\rangle|^2$, is described by

$$\frac{dI_C}{dx}=-\gamma I_C, \tag{11}$$

with the attenuation constant γ. Equatons (10) and (11) lead to the exponential solutions

$$I(x)=I(0)e^{-\alpha x} \quad \text{and} \quad I_C(x)=I(0)e^{-\gamma x}. \tag{12}$$

In deriving these equations, the boundary condition was used; it states that $I(0)=I_C(0)$ as no scattering has been incurred yet at the starting point. According to the energy conservation, the incoherent intensity I_D (diffusive) is thus

$$I_D(x)=I(x)-I_C(x). \tag{13}$$

When there is no absorption, the decay constant α is expected to vanish and the total intensity will then be constant along the propagation path. Then, the coherent energy gradu-

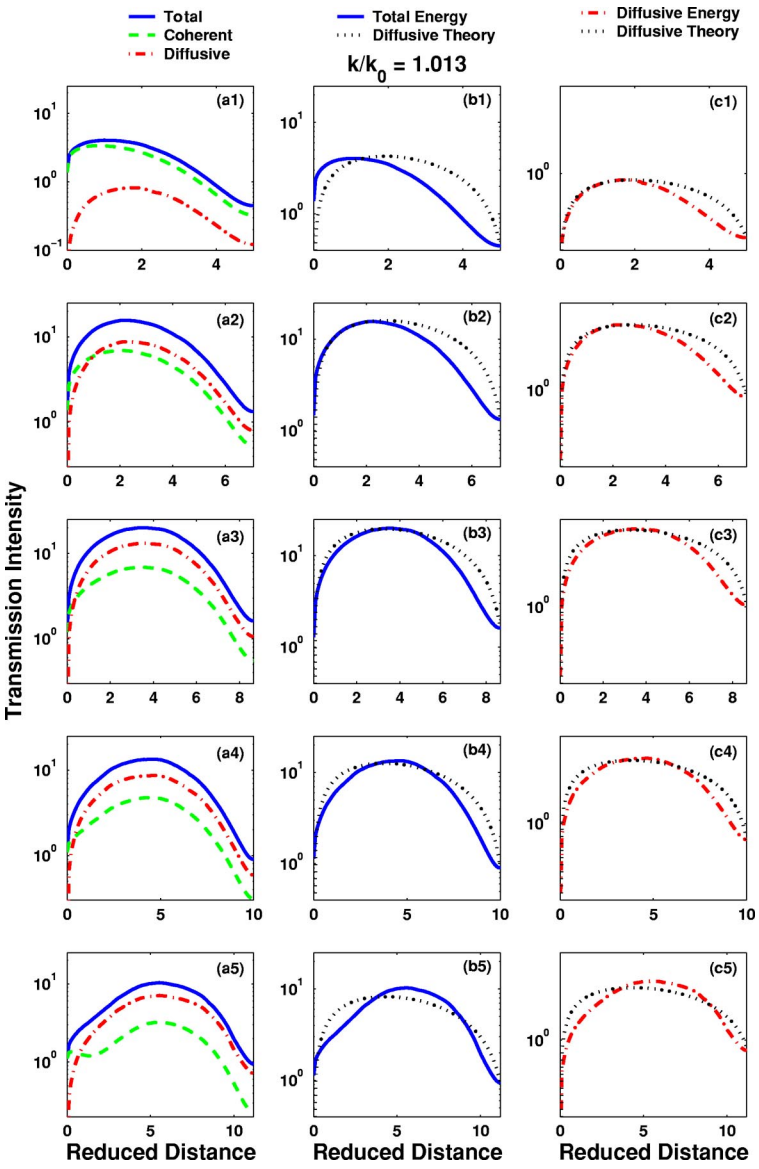

FIG. 4. Dependence of the transport behavior on the sample size for the reduced frequency $k/k_0=1.013$. The following parameters are taken. (1) Diagrams (a1) to (c1): dipole number=491, sample radius=5. (2) Diagrams (a2) to (c2): dipole number=982, sample radius=7. (3) Diagrams (a3) to (c3): dipole number=1473, sample radius=9. (4) Diagrams (a4) to (c4): dipole number=1964, sample radius=10. (5) Diagrams (a5) to (c5): dipole number=2455, sample radius =11. The average has been calculated over 400 random configurations.

ally decreases due to random scattering and transforms to the diffusive energy, while the sum of the two forms of energy remains a constant. This scenario, however, changes when localization occurs. Even without absorption, the total intensity can be localized near the initial point due to multiple scattering. When this happens, α does not vanish. The transport of the total intensity may be still described by Eq. (10), and the inverse of α would then refer to the localization length.

2. Diffusion theory

As discussed above, as waves propagate, the coherent energy gradually decreases and the incoherent (the so-called diffusive waves) progressively grows. In the absence of localization, the diffusive intensity (or energy) will eventually surpasses the coherent energy at a certain point, then becomes the dominating component in the wave transmission. This intuitive physical picture has been nicely phrased in the very excellent textbook by Ishimaru [39].

The diffusive waves are expected to follow the diffusion equation which can be described by

$$\left(D\nabla^2-\frac{\partial}{\partial t}\right)I_D=-S\delta(\vec{r}-\vec{r}_s), \tag{14}$$

where D is the diffusive constant and S denotes a strength factor which is related to the total emitted energy I_0 and transport mean free path l_t. In the steady situation, this equation is simplified as [32,39]

$$\nabla^2 I_D=-\frac{2I_0}{l_t}\delta(\vec{r}-\vec{r}_s). \tag{15}$$

The boundary condition for the diffusive waves is [39]

$$I_D+\frac{2l_t}{3}\frac{\partial I}{\partial n}\bigg|_n=0, \tag{16}$$

with $\vec{n}$ being the outward normal at the boundary.

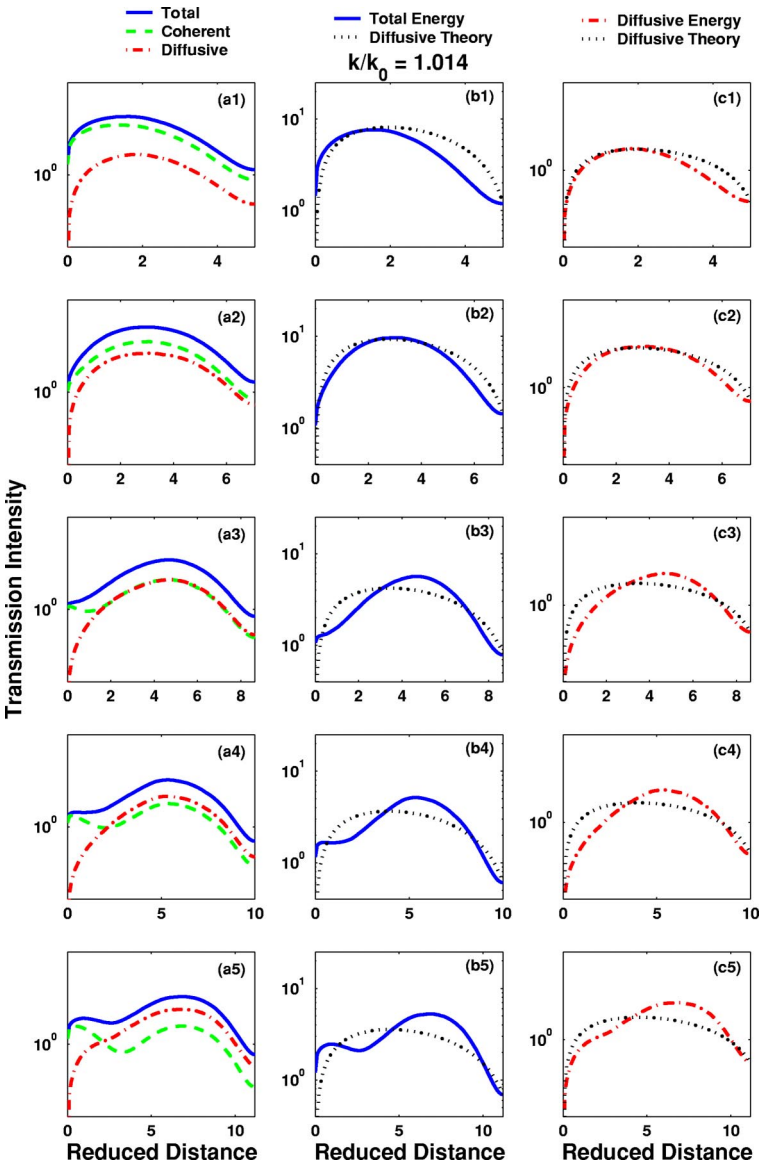

FIG. 5. Dependence of the transport behavior on the sample size for the higher reduced frequency $k/k_0=1.014$. The following parameters are taken. (1) Diagrams (a1) to (c1): dipole number=491, sample radius=5. (2) Diagrams (a2) to (c2): dipole number=982, sample radius=7. (3) Diagrams (a3) to (c3): dipole number=1473, sample radius=9. (4) Diagrams (a4) to (c4): dipole number=1964, sample radius: 10. (5) Diagrams (a5) to (c5): dipole number =2455, sample radius=11. The average has been calculated over 400 random configurations.

As discussed in Ref. [40], the traditional way of measuring for localization effects, that is putting the source at one side of a sample and measuring the transmission across the sample on the other side, may be influenced rather significantly by other nonlocalization effects such as reflection. In the present paper we use an alternative setup in line with the previous studies [32]: Put the source in the middle of a scattering sample which takes a circular shape. In this case, a solution to the diffusive intensity is given as [32]

$$I_D = -\frac{I_0}{\pi l_t}\ln(r/R) + I_b, \tag{17}$$

where R is the sample radius, i.e., the size of the cluster of the scatterers, and I_b is the intensity at the boundary. In practice, l_t can be regarded as a free parameter to fit the numerical simulation. When the diffusive energy is dominant, the total energy would be expected to also follow the behavior characterized by Eq. (17).

III. THE RESULTS AND DISCUSSION

A conceptual set up of the system for discussion is pictured in Fig. 1. Here it is shown that a source is located at the center of a sample circled by the broken line. The small circles inside refer to the dipoles as the scatterers. The receiver is placed at various spatial positions along the radial direction to record the transmitted waves.

A. Parameters in the simulation

Unless otherwise noted, the following parameters are used in the numerical simulation: the nondimensional damping rate $b_0/\omega_0=0.001$ and the interaction coupling $b=0.001$.

In the calculation, we scale all lengths by a unit length l which is chosen such that $k_0 l=1$, and the frequency by ω_0. In this way, the frequency always enters as ω/ω_0 or equivalently k/k_0 and the distance or lengths enter as x/l; both are therefore dimensionless and are called the reduced frequency and reduced distance or length, respectively.

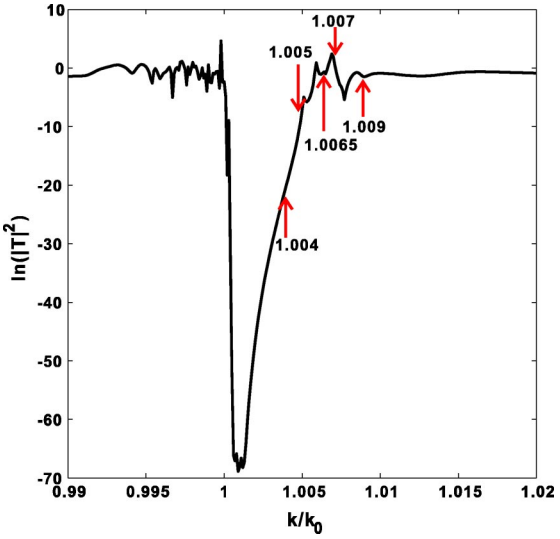

FIG. 6. The transmission vs the reduced frequency. The parameters are as follows. (1) 2150 dipoles in a circular sample, amounting to a sample radius of 15, leading to the filling factor of around 3.00; (2) the receiver is positioned outside at 1.2 radius of the sample.

An important parameter controlling the wave propagation behavior is the number of dipoles per unit area, which is called the filling factor and is denoted by β. As a case study, the filling factor β is taken as about 6.25, i.e., obtained by putting 1964 dipoles within a sample of radius 10 unit length. Without notification, we will use this filling factor. However, some effects due to the variation of the filling factor will also be shown in the later part.

We find that all the results to be shown below are only dependent on parameters b, b_0/ω_0, and the ratio ω/ω_0 or equivalently k/k_0. Such a simple scaling property may facilitate designing experiments. In the numerical computation, we take $c=1$ for convenience. The total normalized wave at a spatial point is scaled as $T(\vec{r}) \equiv E(\vec{r})/E_0(\vec{r})$, with E_0 being the direct wave from the source, so that the trivial geometric spreading effect is naturally removed. When compared with diffusion theory, the diffusive energy would have to be multiplied by the spreading factor, to become $I_D r$. In the simulation, the number of random configurations for averaging is taken in such a way that the convergency is assured.

B. Numerical results and discussion

1. The regime of inhibited transmission

First we plot the wave transmission versus the reduced frequency to locate the strong localization region. The result is shown in Fig. 2. The receiver is located outside at about 1.2 radius of the sample. We see that there is a very strong inhibition region ranging roughly from 1.001 to 1.012. Outside this regime, the inhibition is not obvious. We have tried our current computing facility to its extremes with the largest possible number of dipoles, but we still failed to see obvious inhibition outside the regime. The width of the strong inhibition window mainly depends on the filling factor—the window gets wider and wider monotonically with the increasing filling factor.

2. Transport behavior in general

We choose five frequencies, indicated in Fig. 2, to study the localization or diffusion behaviors of the wave intensity. In Fig. 3, we plot the transmission behavior of various intensities as a function of wave traveling distance for a fixed sample size. The distance has been scaled to be dimensionless by l, as aforementioned. Enough average over the random distributions of the scatterers is taken to ensure the stability of the results; the maximum number of the average is 1200. The observations in Fig. 3 can be summarized as follows.

(1) It is clear from the left panel that within the strong inhibition window, the transmission perfectly follows the expected localization behavior: the total and coherent intensity decays exponentially with slightly different slopes, while the diffusive intensity increases initially, then saturates, followed by a decay afterwards. These are shown by (a1).

(2) As the frequency moves towards the edge of the strong inhibition window, the behavior starts to change more and more severely. As the frequency increases gradually, the total energy starts to behave more like that of diffusive waves, although the diffusive waves are not yet dominant [such as in (a2)]. But overall speaking, the transport behavior of that of total energy behaves more like the diffusive waves when the latter are prominent, as expected and shown by (a3) and (a4).

(3) At frequencies for which the diffusive intensity is dominant, the behavior of the diffusive energy is qualitatively in agreement with the prediction of the diffusion theory, such as in the cases described by (c3), but in certain cases the agreement is good both qualitatively and quantitatively as seen in (c4). Generally speaking, however, the agreement is less encouraging compared with the simulation for another 2D system illustrated in Ref. [32]. And the rapid fluctuation of the diffusive energy shown in Ref. [32] is absent here. Another note is worth making here. In Ref. [32], the authors also compared the results within a strong localization region. The exponential decay revealed in their figures, for example Fig. 9, is only possible when the cylindrical geometrical spreading factor $1/r$ is taken out. It seems to us that this factor may not have been considered in their discussion.

(4) Just by looking, we are tempted to conclude that there is indeed a fundamental difference in the transport behaviors between within and outside the strong inhibition region. This phenomenon accords qualitatively with the observation in Ref. [32].

(5) We also observe that outside the strong inhibition regime, the coherent intensity does not necessarily behave as an exponential decay, exemplified by (a3) and (a4). This is in contrast to usual expectation. A plausible cause is the finite size effects which are unavoidable due to the limitation of the computing facilities. In fact, the waves can be reflected at the interface between the free space and the spatial domain filled with the dipoles, and the reflected waves thus contribute to the intensities inside the sample. In this situation, the mean free path is hard to estimate, unlike in other systems [29,40].

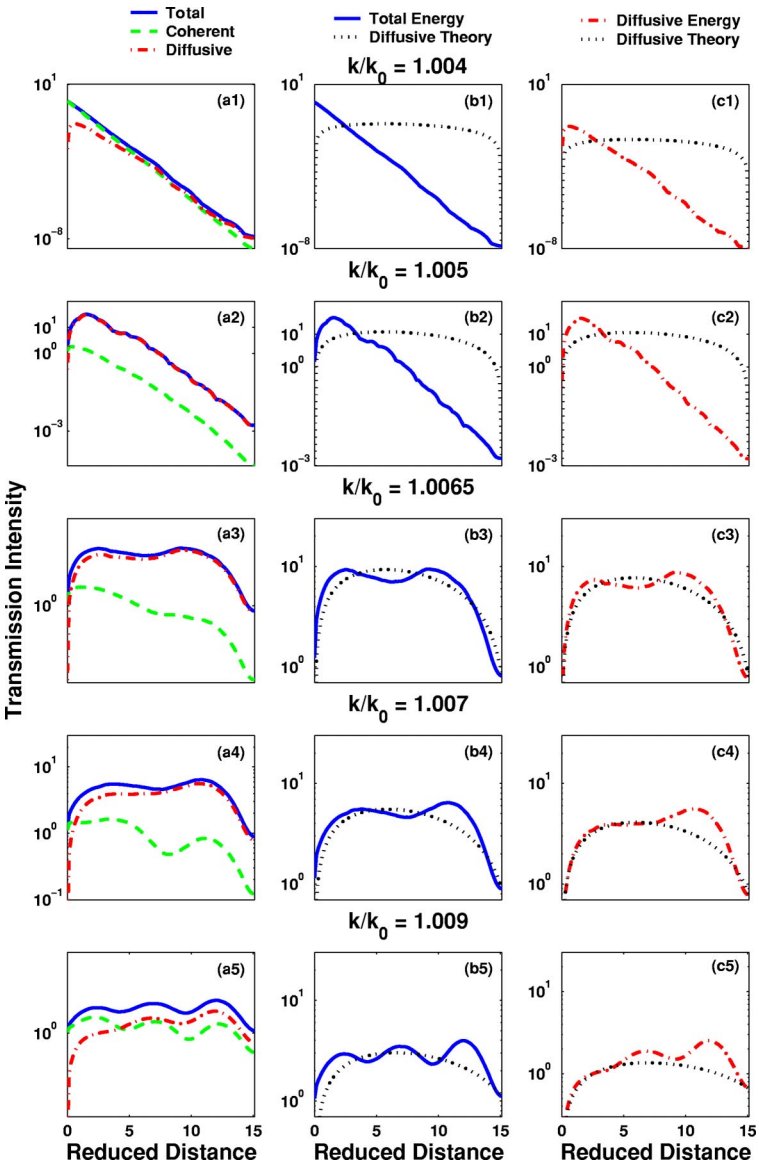

FIG. 7. Transport behavior: (a) the total, coherent, and diffusive intensity as a function of the reduced traveling distance; (b) the comparison of the numerical results of the total energy with that from the diffusion theory; (c) the comparison of the numerical results of the diffusive energy with that from the diffusion theory. We considered 2150 dipoles to form a sample whose radius is 15, in accordance with Fig. 6.

3. Sample size and frequency effects

From Fig. 3, we see that at around $k/k_0=1.013$, just outside the upper edge of the strong localization boundary, the diffusive waves are dominant and the transport behavior tends to follow the prediction from the diffusion theory. Now we would like to explore the robustness of such an agreement as the sample size and frequency vary.

The results of the sample size effects are shown in Fig. 4. Here it shows that as the size of the sample, in terms of the sample radius, is increased, the diffusive intensity becomes more and more prominent, meanwhile the agreement between the diffusion and exact numerical results is improved, as shown by the diagrams from the top downwards. However, there is always some discrepancy between the simulation and theoretical results. The reason why we have taken five sample sizes for discussion is purely to show the gradual improvement in the agreement.

When we consider another close frequency $k/k_0=1.014$, the agreement does not seem to improve as the sample size is enlarged. The comparison is shown in Fig. 5. The best agreement is when the sample size is 7, referring to (b2) and (c2). From these results, one may say that the agreement between the diffusion theory and the exact numerical results may not be robust, at least in the present system. We have to note that the results from the diffusion theory are approximate. The deviation from the diffusion theory is therefore not out of expectation.

4. Different filling factor

We also considered the case for a smaller filling factor at about 3.00. The general features are agreeable with the above case with 6.26. For brevity, we just show partial results. Figure 6 shows the transmission versus the reduced frequency. The parameters are given in the figure caption. Compared to the case with filling factor of 6.25, we see that decreasing filling factor only tends to reduce the strong inhibition regime while all other features remain more or less the same, as compared to Fig. 2.

Again we choose five frequencies to inspect the transport behavior, and show the results in Fig. 7. The general conclu-

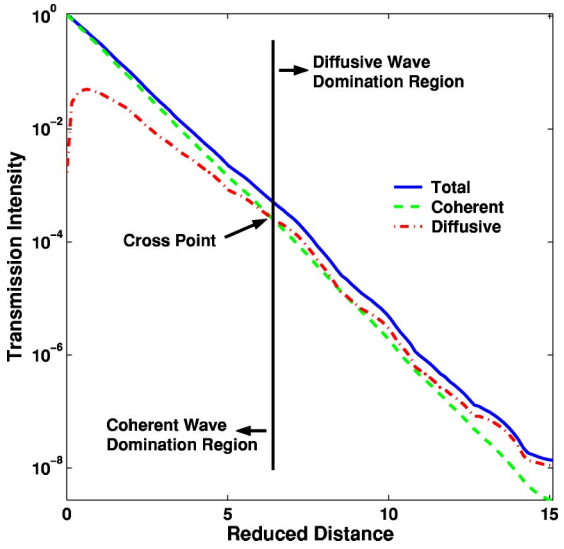

FIG. 8. Replotted results of Fig. 7(a1).

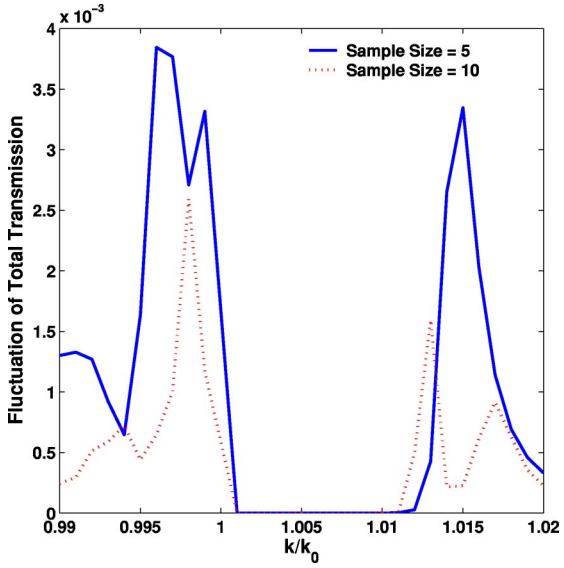

FIG. 9. The fluctuation of the normalized transmission intensity, i.e., $\delta T^2 = \langle T^2 \rangle - \langle T \rangle^2$, vs the reduced frequency.

sions drawn from Fig. 3 remain qualitatively unchanged. However, there are differences. For the frequency 1.004 which is within the strong localization regime, the transport behavior fully complies with the expectation. The diffusive intensity increases, saturates, and then decreases, while taking over as the dominating part in the total transmission. We replot Fig. 7(a1) in Fig. 8 to show this behavior. The cross over point at which the diffusive part becomes dominating is represented by the vertical line in the figure.

5. Fluctuation behavior in the transmission

Finally, we have computed the fluctuation of the normalized transmission intensity versus the reduced frequency. The results are shown in Fig. 9. The parameters are as follows: filling factor (number of dipole/area)=6.25; two sample sizes are 5 and 10, respectively; the receiver is at 1.2 times the radius of the sample; and the number of average is 100. The results indicate that the fluctuation is nearly zero within the localization regions. Outside these regimes, the fluctuation is comparatively strong. The results also show that the localization regime is the same for different sample sizes. These features hint that there may be a localization transition in 2D random media, in accordance with the previous results [31,32].

IV. SUMMARY

In this paper, we have discussed the transport properties of electromagnetic waves in a two-dimensional random system. Some general properties of the transport phenomena are elaborated. For certain ranges of frequencies, strongly localized electromagnetic waves have been observed in such a system. The spatial behavior of the total, coherent, and diffusive waves is explored within, near the edge of, and outside the localization regime, and is investigated for different parameters such as filling factor and system size.

The results show that within the localization regime, waves are trapped near the transmitting source. Meanwhile, the diffusive waves follow an intuitive but expected picture. For the cases that the frequencies are near the boundary of or outside the localization regime, the results of diffusive waves are compared with the diffusion approximation, showing less encouraging agreement as in other systems [32]. Furthermore, the results tend to suggest that the study of the fluctuation behavior in the transmission may also help identify the localization regime.

ACKNOWLEDGMENTS

This work was supported by the National Science Council of Republic of China (Grant No. 91-2112-M008-024). Support from Department of Physics, College of Science, and the National Central University is also greatly appreciated. Without this help, the simulation carried out here would be impossible.

[1] P.W. Anderson, Phys. Rev. **109**, 1492 (1958).
[2] P.A. Lee and Ramakrishnan, Rev. Mod. Phys. **57**, 287 (1985).
[3] J.D. Maynard, Rev. Mod. Phys. **73**, 401 (2001).
[4] R. Hennino *et al.*, Phys. Rev. Lett. **86**, 3447 (2001).
[5] G.I. Barenbatt, M.E. Vinogradov, and S.V. Petrovskii, Oceanology (Engl. Transl.) **35**, 202 (1995).
[6] Z.Q. Zhang, Phys. Rev. B **52**, 7960 (1995); S. Wiersma, M.P. van Albada, and A. Lagendijk, Nature (London) **373**, 203 (1997); H. Cao *et al.*, Phys. Rev. Lett. **82**, 2278 (1999); C.M. Soukoulis, X. Jiang, J.Y. Xu, and H. Cao, Phys. Rev. B **65**, 041103 (2002).
[7] D.J. Thouless, Phys. Rep. **13**, 93 (1974).

[8] S. John, Phys. Today **44**(5), 52 (1991).
[9] P. Sheng, *Introduction to Wave Scattering, Localization, and Mesoscopic Phenomena* (Academic Press, New York, 1995).
[10] A. Lagendijk and B.A. van Tiggelen, Phys. Rep. **270**, 143 (1996).
[11] B.A. van Tiggelen, *Diffuse Waves in Compex Media* (Kluwer Academic Publisher, Netherlands, 1999).
[12] M.C.W. van Rossum and Th.M. Nieuwenhuizen, Rev. Mod. Phys. **71**, 313 (1999).
[13] M. Janssen, *Fluctuations and Localization* (World Scientific, Singapore, 2001), and references therein.
[14] C.H. Hodges and J. Woodhouse, J. Acoust. Soc. Am. **74**, 894 (1983).
[15] T.R. Kirkpatrick, Phys. Rev. B **31**, 5746 (1985).
[16] S. He and J.D. Maynard, Phys. Rev. Lett. **57**, 3171 (1986).
[17] C.A. Condat, J. Acoust. Soc. Am. **83**, 441 (1988).
[18] D. Sornette and B. Souillard, Europhys. Lett. **7**, 269 (1988).
[19] A.Z. Genack and N. Garcia, Phys. Rev. Lett. **66**, 2064 (1991).
[20] R. Dalichaouch, J.P. Armstrong, S. Schultz, P.M. Platzman, and S.L. McCall, Nature (London) **354**, 53 (1991).
[21] S.L. McCall, P.M. Platzman, R. Dalichaouch, D. Smith, and S. Schultz, Phys. Rev. Lett. **67**, 2017 (1991).
[22] M. Rusek and A. Orlowski, Phys. Rev. E **51**, R2763 (1995).
[23] M.M. Sigalas, C.M. Soukoulis, C.-T. Chan, and D. Turner, Phys. Rev. B **53**, 8340 (1996).
[24] A.A. Asatryan *et al.*, Phys. Rev. B **57**, 13 535 (1998).
[25] Z. Ye and A. Alvarez, Phys. Rev. Lett. **80**, 3503 (1998).
[26] Y. Kuga and A. Ishimaru, J. Opt. Soc. Am. A **1**, 831 (1984); M. van Albada and A. Lagendijk, Phys. Rev. Lett. **55**, 2692 (1985); P.E. Wolf and G. Maret, Phys. Rev. Lett. **55**, 2696 (1985); A. Tourin *et al.*, *ibid.* **79**, 3637 (1997); M. Torres, J.P. Adrados, and F.R. Montero de Espinosa, Nature (London) **398**, 114 (1999).
[27] D.S. Wiersma, P. Bartolini, A. Lagendijk, and R. Roghini, Nature (London) **390**, 671 (1997).
[28] A.A. Chabanov, M. Stoytchev, and A.Z. Genack, Nature (London) **404**, 850 (2000).
[29] X. Zhang and Z.Q. Zhang, Phys. Rev. B **65**, 155208 (2002).
[30] E. Abrahams, P.W. Anderson, D.C. Licciardello, and T.V. Ramakrishnan, Phys. Rev. Lett. **42**, 673 (1979).
[31] E. Hoskinson and Z. Ye, Phys. Rev. Lett. **83**, 2734 (1999).
[32] A.A. Asatryan *et al.*, Phys. Rev. E **67**, 036605 (2003).
[33] Z. Ye, S. Li, and X. Sun, Phys. Rev. E **66**, 045602(R) (2002).
[34] T. Erdogan, K.G. Sullivan, and D.G. Hall, J. Opt. Soc. Am. B **10**, 391 (1993).
[35] K. Wang and Z. Ye, cond-mat/0302596.
[36] C.-C. Wang and Z. Ye, Phys. Status Solidi A **174**, 527 (1999).
[37] R. Zallen, *The Physics of Amorphous Solids* (Wiley, New York, 1983).
[38] Z. Ye, H.-R. Hsu, E. Hoskinson, and A. Alvarez, Chin. J. Phys. (Taipei) **37**, 343 (1999).
[39] A. Ishimaru, *Wave Propagation and Scattering in Random Media* (Academic Press, New York, 1978).
[40] Y.-Y. Chen and Z. Ye, Phys. Rev. E **65**, 056612 (2002).